Title

Fluorescence photooxidation with eosin: a method for high resolution immunolocalization and in situ hybridization detection for light and electron microscopy.

Journal

Journal of Cell Biology, 126(4)

ISSN

0021-9525

Authors

Deerinck, TJ
Martone, ME
Lev-Ram, V
et al.

Publication Date

1994-08-15

DOI

10.1083/jcb.126.4.901

Peer reviewed

Fluorescence Photooxidation with Eosin: A Method for High Resolution Immunolocalization and In Situ Hybridization Detection for Light and Electron Microscopy

Thomas J. Deerinck, Maryann E. Martone, Varda Lev-Ram,* David P. L. Green,* Roger Y. Tsien,‡ David L. Spector,§ Sui Huang,§ and Mark H. Ellisman

Microscopy and Imaging Resource, *Department of Pharmacology, and ‡Howard Hughes Medical Institute, University of California, San Diego, La Jolla, California 92093-0608; §Cold Spring Harbor Laboratory, Cold Spring Harbor, New York 11724

Abstract. A simple method is described for high-resolution light and electron microscopic immunolocalization of proteins in cells and tissues by immunofluorescence and subsequent photooxidation of diaminobenzidine tetrahydrochloride into an insoluble osmiophilic polymer. By using eosin as the fluorescent marker, a substantial improvement in sensitivity is achieved in the photooxidation process over other conventional fluorescent compounds. The technique allows for precise correlative immunolocalization studies on the same sample using fluorescence, transmitted light and electron microscopy. Furthermore, because eosin is smaller in size than other conventional markers, this method results in improved penetration of labeling reagents compared to gold or enzyme based procedures. The improved penetration allows for three-dimensional immunolocalization using high voltage electron microscopy. Fluorescence photooxidation can also be used for high resolution light and electron microscopic localization of specific nucleic acid sequences by in situ hybridization utilizing biotinylated probes followed by an eosin-streptavidin conjugate.

FLUORESCENT labeling techniques have become increasingly popular in many areas of cell biology, particularly due to the expanded use of laser scanning confocal microscopy. Immunofluorescent localization of proteins and fluorescence-based in situ hybridization detection of specific nucleic acid sequences in cells and tissues have several advantages over other labeling procedures including relative simplicity, shorter processing times, high sensitivity, and good spatial resolution. One of the major disadvantages of fluorescent labeling has been the inability to use this technique for correlated light and electron microscopic studies in cases requiring better than light microscopic resolution. Several methods have been introduced in an attempt to overcome this limitation. These include the use of anti-fluorophore antibodies, e.g., anti-fluorescein, conjugated to peroxidase (Peters et al., 1990) and the process of fluorescence photooxidation of diaminobenzidine (DAB).[1] This latter method, first described by Maranto (1982), involves the use of fluorescent dyes to oxidize DAB into an insoluble reaction product.

Photooxidation represents a relatively simple method to render fluorescently labeled preparations suitable for electron microscopic examination. Briefly, a fluorescent dye is excited in the presence of DAB and gradually an oxidized DAB reaction product forms. The reaction product is highly insoluble and easily visible with ordinary transmitted light microscopy. Since the DAB reaction product is osmiophilic, this technique can be used for correlative light and electron microscopic studies using a variety of fluorescent compounds including Lucifer yellow, DiI, Bodipy ceramide, fluorogold, and fluororuby (Pagano et al., 1989; Bentivoglio and Su, 1990; von Bartheld et al., 1990; Balercia et al., 1992; Lubke, 1993; Papadopoulos and Dori, 1993; Schmued and Snavely, 1993; Takizawa et al., 1993). A potentially powerful application of this technique is for correlated light and electron microscopic studies of immunolabeled specimens. Although photooxidation of DAB by fluorescein and rhodamine has been reported in immunolabeled cultured cells (Sandell and Masland, 1988), our attempts at photooxidation using these conventional fluorophores have not been satisfactory in terms of either sensitivity or spatial resolution. Even with intense fluorescent immunolabeling using fluorescein-conjugated antibodies, very little photooxidation was observed.

Given the poor performance of fluorescein and rhodamine in this reaction, we sought other fluorescent compounds that

Address all correspondence to M.H. Ellisman, Ph.D., Microscopy and Imaging Resource, University of California, San Diego, La Jolla, CA 92093-0608.

D.P.L. Green's permanent address is Department of Pharmacology, University of Otago, Dunedin, New Zealand.

1. *Abbreviations used in this paper*: CSB, cytoskeleton stabilizing buffer; DAB, diaminobenzidine.

would be more efficient photooxidizers. Since the production of reactive oxygen species by the fluorophore has been implicated in the photooxidation reaction (Sandell and Masland, 1988), we tested fluorescent compounds that were more potent generators of singlet oxygen. Many of the compounds currently used for immunofluorescent labeling such as fluorescein and rhodamine were chosen because of their high fluorescence quantum yields (Φ_f), and have comparatively low yields of singlet oxygen ($^1O_2$). Eosin, a brominated derivative of fluorescein, has a singlet oxygen quantum yield (Φ_{1O_2}) approximately 19 times greater than fluorescein (Gandin et al., 1983), while still possessing moderate fluorescence (~20% as bright as fluorescein) (Fleming et al., 1977). We found that eosin conjugated via its 5-isothiocyanate derivative to secondary anti-immunoglobulin antibodies or to streptavidin could be used for both high quality immunofluorescence imaging and for the efficient photooxidation of DAB for subsequent electron microscopic examination. The improvement in photooxidation efficiency achieved with eosin not only allows this technique to be used for immunolabeling, but also makes it suitable for fluorescence in situ hybridization detection. Furthermore, following osmification the photooxidized DAB reaction product exhibits exceptionally uniform staining characteristics with little granularity, making it suitable for use in localization studies requiring high resolution. We describe here a method that uses eosin-conjugated reagents for the correlated light and electron microscopic immunolocalization of proteins as well as in situ hybridization detection of specific nucleic acid sequences.

Materials and Methods

Materials

Eosin-5-isothiocyanate and streptavidin were obtained from Molecular Probes (Eugene, OR). Affinity purified goat anti-rabbit and goat anti-mouse IgG was obtained from Jackson ImmunoResearch Labs., Inc. (West Grove, PA). 3,3'diaminobenzidine tetrahydrochloride and cold water fish gelatin were obtained from Sigma Immunochemicals (St. Louis, MO). Paraformaldehyde, EM grade glutaraldehyde, sodium cacodylate, and Durcopan ACM resin were obtained from Electron Microscopy Sciences (Fort Washington, PA). Special welled tissue culture plates were obtained from MatTek (Ashland, MA). Cell-Tak adhesive was obtained from Collaborative Research Inc. (Bedford, MA). The anti-β-tubulin antiserum was a gift of Dr. Richard McIntosh (University of Colorado, Boulder, CO) and the anti-calsequestrin antiserum was a gift of Dr. John Sutko (University of Nevada, Reno, NV).

Conjugation of Eosin to IgG and Streptavidin

Conjugation of eosin to IgG was carried out using a protocol supplied by Molecular Probes Inc. Briefly, 20 mg of goat anti-rabbit or goat anti-mouse IgG was dissolved in 0.8 ml of 0.1 M sodium bicarbonate, pH 9.0. Eosin-5-isothiocyanate, dissolved in 100 μl of dimethylformamide at a final concentration of 1.25 mM, was added to the IgG solution while stirring and allowed to incubate at room temperature for 1 h. The reaction was stopped by adding 0.1 ml of freshly prepared 1.5 M hydroxylamine, pH 8.0, and incubating for 30 min. The conjugate was separated from the unreacted labeling reagent on a gel filtration column of sephadex G-25 equilibrated with 0.1 M PBS. The conjugate was dialyzed overnight in dialysis bags (cut off 8–9 kD) against PBS at 4°C. A dye/protein ratio of 3:1 gave good staining results for both the mouse and rabbit IgG. Absorption maxima were determined with a diode-array Lambda 3840 UV/VIS spectrophotometer (Perkin-Elmer Corp., Norwalk, CT). Emission maxima were determined with a Fluorolog Spex 1681 spectrometer.

The same procedure was used to conjugate eosin to streptavidin. A dye/protein ratio of 2:1–4:1 gave good staining results.

Spectrophotometric Analysis

To examine various aspects of the photooxidation reaction in a controlled system, cuvette experiments were performed in which the rate and amount of photooxidation were monitored using a diode-array spectrophotometer (Perkin-Elmer Corp.). DAB photooxidation could be measured in solution as an increase in OD across a broad spectrum from 350 to 650 nm. Reactions were run in a 10 by 10 mm quartz cuvette illuminated from the side using a xenon arc lamp focused on the cuvette. This actinic light path was shuttered and routinely contained a short pass filter (<650 nm) to remove the infrared (a copper sulfate solution) and a long pass filter (>420 nm) to remove UV light. Additional band pass filters were inserted for comparing the efficiency of fluorescein and eosin in the photooxidation and for the estimate of quantum yield. Assay solutions contained DAB from an 800 mM stock solution in dimethylsulfoxide. Dilutions of DAB were made in 0.2 M Hepes buffer, pH 7.0, and the fluorescent dye. Solutions were bubbled with either argon (to displace oxygen) or air throughout each experiment. This also provided mixing of the cuvette contents.

The cuvette setup was used to assess the effects of DAB and eosin concentration on photooxidation, to compare the photooxidation efficiency of various dyes, to estimate the approximate quantum yield for the eosin-induced photooxidation reaction, and to investigate possible reaction mechanisms. Eosin and fluorescein were compared in the photooxidation reaction using band pass filters at 515 and 488 nm, respectively. These filters had identical transmittances and half-height band widths. The concentrations of dyes (54 μM fluorescein and 29 μM eosin) were chosen to ensure essentially complete light absorption.

The quantum yield of eosin photooxidation was also measured using a band pass filter (515 nm) for the actinic light path. It was assumed that where the ΔOD reaches a plateau, the conversion of DAB to polymer was complete and had consumed all available DAB. Since the initial DAB concentration was known, the absolute rate of DAB conversion was calculated for the early part of the OD vs. time curve. The intensity of the light falling on the sample was measured by chemical actinometry using the ferrioxalate method (Hatchard et al., 1956).

Immunolabeling of Cultured Cells

Bovine aortic endothelial cells were cultured according to Galbraith (Galbraith, 1994). Cells were grown on special tissue culture dishes (MatTek Inc.) incorporating a coverslip on the bottom to facilitate visualization with an inverted microscope. Cells were fixed in 1% formaldehyde (from paraformaldehyde) and 0.05% glutaraldehyde in cytoskeleton stabilizing buffer (CSB) (Conrad et al., 1989), pH 6.8, for 10 min. Cells were washed in CSB for 15 min, permeabilized in 0.5% Triton X-100 in CSB with 0.05 M glycine (CSB-gly) for 1.5 min, and then washed for 15 min in CSB. Nonspecific binding was blocked with 0.5% cold water fish gelatin, 0.5% bovine serum albumin, and 1% normal goat serum in CSB-gly. Following 30 min of washing, the cells were incubated in monoclonal anti-β tubulin antiserum for 1 h. Cells were washed for another 30 min and then incubated with goat anti-mouse IgG-eosin conjugate for 1 h.

Immunolabeling of Tissue Sections

Hatchling leghorn chicks were anesthetized deeply with Nembutal and perfused transcardially with normal rat Ringer's at 35°C followed by 4% formaldehyde (made fresh from paraformaldehyde) in 0.15 M sodium cacodylate, pH 7.4. The cerebellum was removed and fixed an additional 1 h in the same solution at 4°C. Sections were cut at a thickness of 50–100 μm with a Vibratome, rinsed in 0.15 M cacodylate, and then incubated for 30 min in 1% normal goat serum, 1% bovine serum albumin, and 1% cold water fish gelatin and 0.05% saponin in 0.15 M cacodylate to block nonspecific binding. The sections were incubated in primary antibody for 12 h, washed in buffer and incubated an additional hour in goat anti-rabbit or goat anti-mouse IgG–eosin conjugate. After additional washes, the sections were mounted on welled tissue culture dishes (MatTek Inc.) pretreated with Cell-Tak adhesive to hold them in place during confocal imaging and photooxidation.

In Situ Hybridization

HeLa cells were grown on special culture dishes (MatTek) in DME supplemented with 10% fetal calf serum (GIBCO BRL, Gaithersburg, MD) and maintained at 37°C with 7.5% CO_2. Cells were fixed in 4% paraformaldehyde containing 0.01% glutaraldehyde for 15 min at room temperature. An oligo $dT_{(50)}$ was 3' end labeled with biotin and used as a probe for

in situ hybridization to poly(A)$^+$ RNA. The hybridization mixture contained 4 ng/l of probe, 2× SSC, 1 mg/ml of tRNA, 10% dextran sulphate, and 25% formamide. Hybridization was performed at 42°C in a humidified chamber overnight. After hybridization, cells were washed twice for 15-min each in 2× SSC, and 15 min in 0.5× SSC. Cells were rinsed in PBS and incubated for 1–2 h in streptavidin–eosin conjugate, followed by brief washes in PBS. As with many other fluorophores, eosin conjugated to streptavidin exhibited partial fluorescence quenching, presumably due to interactions with amino acid residues in the biotin-binding region of streptavidin. This phenomenon was significantly reduced by adding free biotin (20 μM) as a final step in the labeling process, thereby greatly improving the fluorescence brightness of the conjugate.

Fluorescence Imaging

Fluorescence microscopy was performed on a Zeiss Axiovert 35 M using either a 63× 1.4 NA or 40× 1.3 NA objective lens. Fluorescent and transmitted light images were recorded using a laser scanning confocal attachment (MRC-600; Bio-Rad Laboratories, Cambridge, MA) using either an argon or krypton/argon laser. During observation it was important to use a deoxygenated buffer solution to retard photobleaching. This was achieved by bubbling the solution with argon gas for several minutes.

Photooxidation

After fluorescence images were recorded, the cultured cells or tissue sections were again fixed for 5–10 min with 2% glutaraldehyde in 0.1 M cacodylate buffer, rinsed in buffer for several minutes, and then treated with 100 mM glycine in buffer for an additional 5 min to reduce nonspecific staining. In some instances, treatment for several minutes with 6 mM potassium cyanide was used to reduce oxidation of DAB by mitochondria. The samples were then immersed in a chilled (~4°C) solution of 2.8 mM DAB in 0.1 M sodium cacodylate bubbled with pure O_2 , final pH 7.4, and irradiated using 515 ± 10 nm excitation from either a 100 or 200 W mercury or 75 W xenon arc light source. Continuous observations were made during the photooxidation procedure using transmitted light. Under these conditions the fluorescence faded very quickly, and after several minutes a brownish reaction product began to appear in place of the fluorescence. The process was stopped by halting the excitation.

Postphotooxidation Processing

Following photooxidation the cells or tissue sections were rinsed in 0.1 M sodium cacodylate several times and treated for 30 min with 2% osmium tetroxide in 0.1 M sodium cacodylate. After several washes with H_2O, the samples were dehydrated in an ethanol series, infiltrated with Durcopan ACM resin, and polymerized for 24 h at 60°C.

Electron Microscopy

Sections were cut with a Reichert Ultracut E at a thickness of 80 nm using a diamond knife and examined using either a JEOL 100CX or 2000EX electron microscope at 80 keV. Thicker sections (0.25–1.0 μm) were examined with a JEOL 4000EX at 400 keV. Stereopairs were generated by tilting the specimen 12° between micrographs.

Results

Eosin-5-isothiocyanate (705 mol wt) is structurally identical to fluorescein-5-isothiocyanate except for the addition of four bromine atoms (Fig. 1 *A*). It exhibits moderate fluorescence and good photostability as compared to fluorescein. When conjugated to immunoglobulins by standard methods it has a measured absorption maxima at 526 nm and emission maxima at 545 nm (Fig. 1 *B*). Eosin conjugated to either an IgG or steptavidin can be used in conventional immunofluorescent staining protocols and has also been proposed as an alternative to fluorescein when performing con-

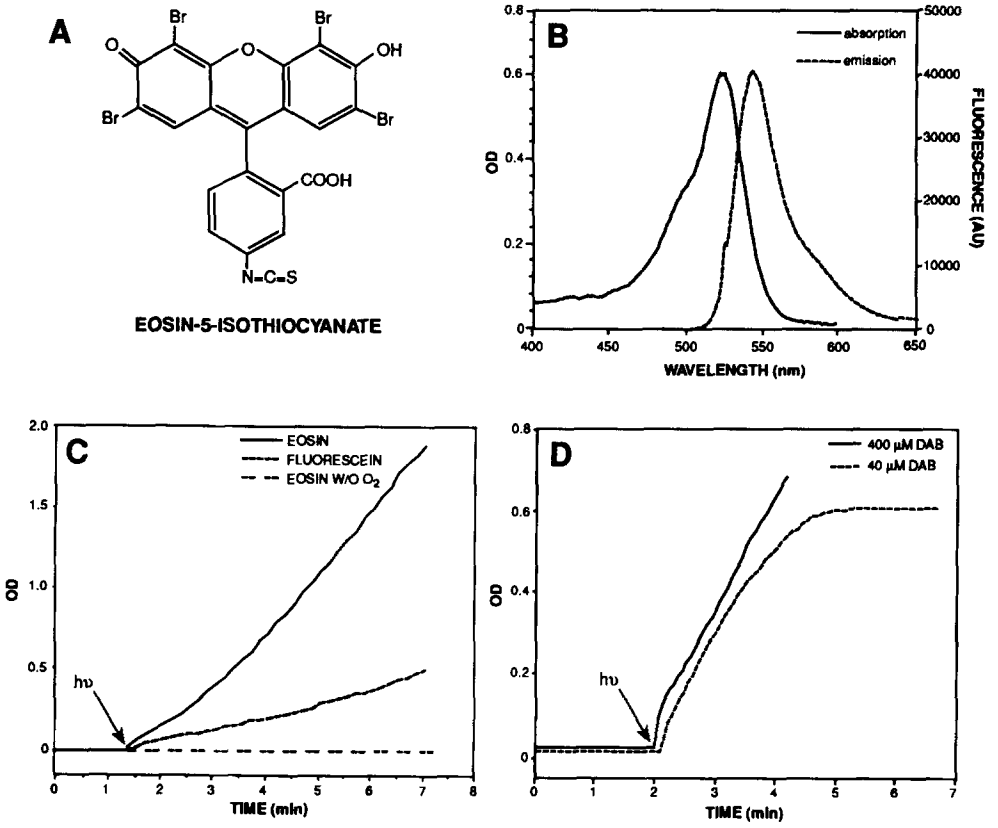

Figure 1. (*A*) The molecular structure of eosin-5-isothiocyanate is shown. It is essentially identical to fluorescein-5-isothiocyanate except for addition of four bromine atoms. The addition of these atoms significantly increases the nonfluorescent dissipation of energy from the excited dye molecule through intersystem crossing, making it a potent generator of singlet oxygen. (*B*) The absorption and emission spectra of an eosin-IgG conjugate. The eosin conjugate exhibits an absorption maxima at 526 nm and an emission maxima at 545 nm. (*C*) Comparison of photooxidation rates of DAB in the presence of either unconjugated fluorescein or eosin. Under comparable conditions, the rate of photooxidation with eosin is significantly faster than with fluorescein. If oxygen is displaced with argon, the reaction is completely inhibited. Starting OD's were adjusted to zero. (*D*) Reaction rates for 40 μM vs 400 μM DAB in the presence of 5 mM eosin. A plateau is reached with 40 μM DAB, suggesting complete depletion of DAB monomer. Increasing the concentration of DAB 10-fold has no effect on the rate, indicating rapid scavenging of DAB by the reactive species at both DAB concentrations.

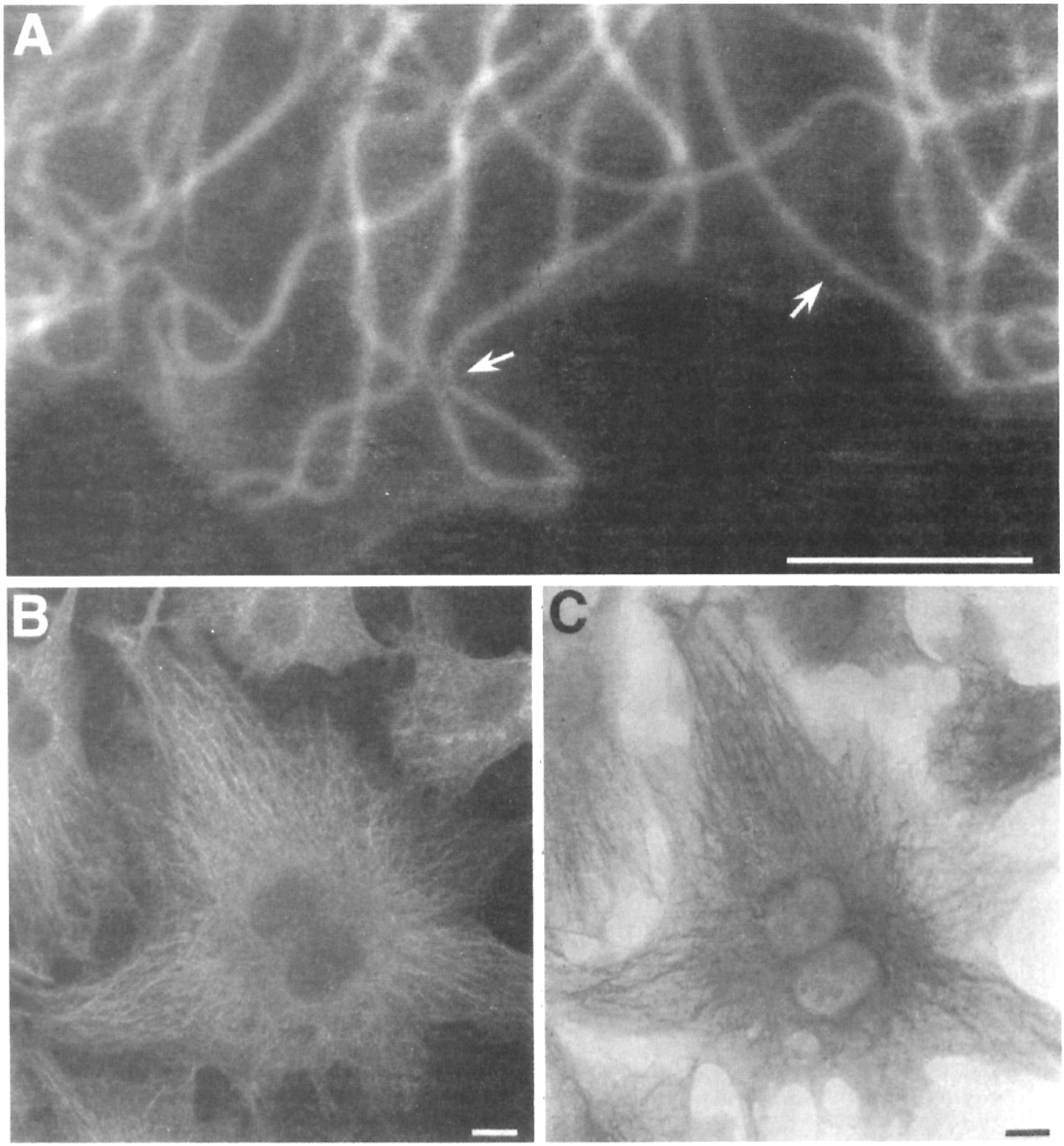

Figure 2. (*A*) High magnification laser scanning confocal image of microtubules in the peripheral portion of a bovine aortic endothelial cell labeled with mouse anti-β tubulin antibodies followed by a goat anti-mouse eosin conjugate. (*B*) A low power fluorescence image of cells stained as in *A* immediately prior to photooxidation. (*C*) The same region viewed with transmitted light following photooxidation. Note the correspondence of the staining patterns. Bars: (*A*) 2 μm; (*B* and *C*) 5 μm.

focal microscopy with 514-nm excitation from an argon laser (Hulspas et al., 1993).

To compare the relative efficiencies of various fluorescent compounds in photooxidizing DAB, an in vitro–based reaction apparatus was developed. This consisted of a light source and cuvette coupled to a diode-array spectrophotometer used to measure the relative OD of the DAB solution. Under conditions in which there was complete light absorption and the initial DAB concentrations were identical, eosin was significantly more effective than fluorescein in the photooxidation of DAB (Fig. 1 *C*). An estimate of the photooxidative quantum efficiency was made by taking advantage of the fact that apparent exhaustion of DAB monomer gave a stable plateau after photooxidation (Fig. 1 *D*). If it was as-

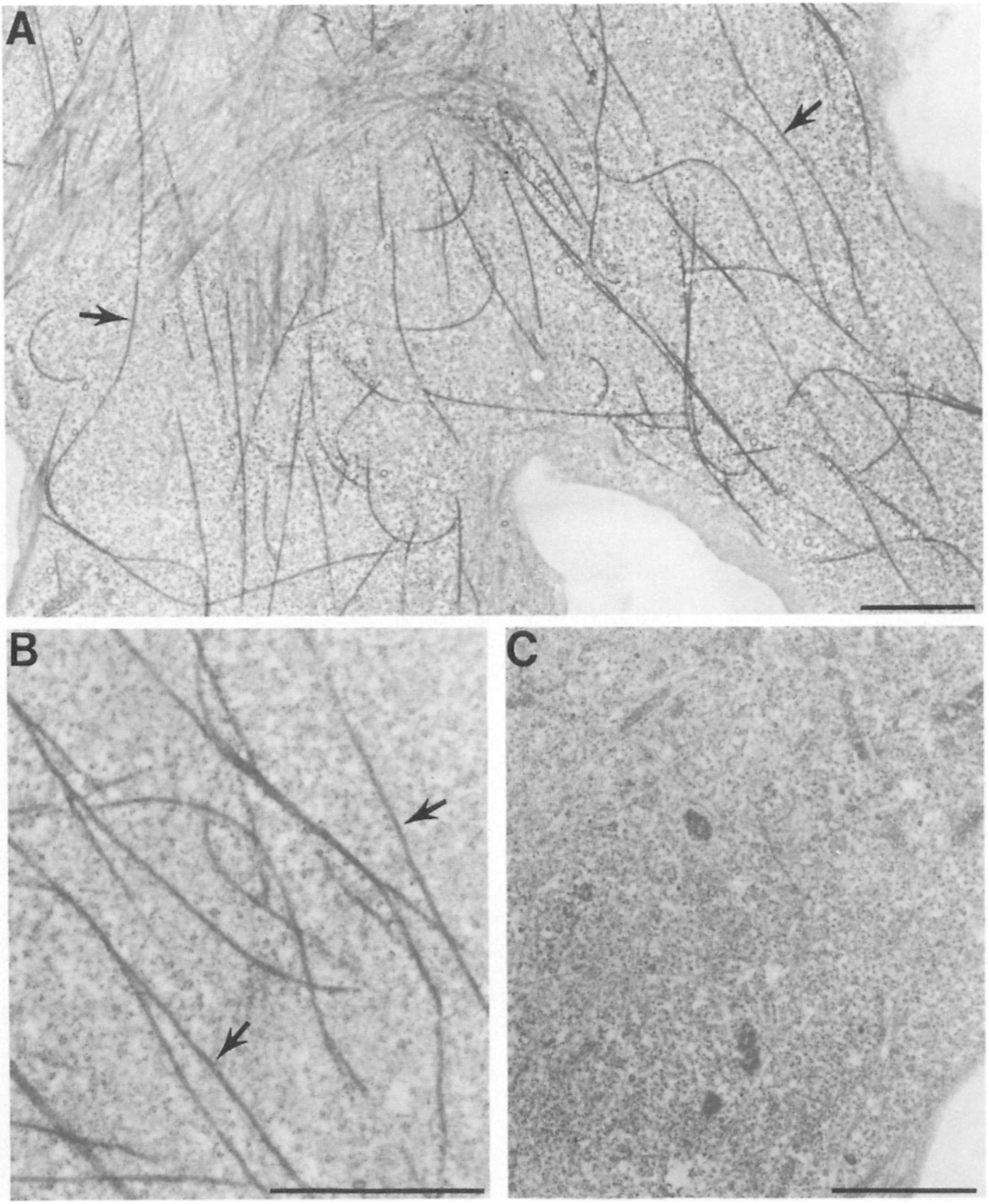

Figure 3. (*A* and *B*) Electron micrograph of a cell labeled for β-tubulin followed by photooxidation with eosin. The specific staining of individual microtubules can be seen (*arrows*). (*C*) A region of a cell from the same culture plate beyond the field of illumination. No microtubule labeling is evident. Bar, 2 μm.

sumed that this plateau did indeed represent complete loss of DAB monomer, and that the initial increase in OD on illumination represented the stoichiometric loss of DAB monomer, then the absolute number of DAB molecules oxidized per unit time could be related to the number of photons entering the cuvette. Using these assumptions, it was calculated that ~15% of photons absorbed by eosin resulted in the photooxidation of DAB molecules by eosin. Fig. 1 *D* also shows

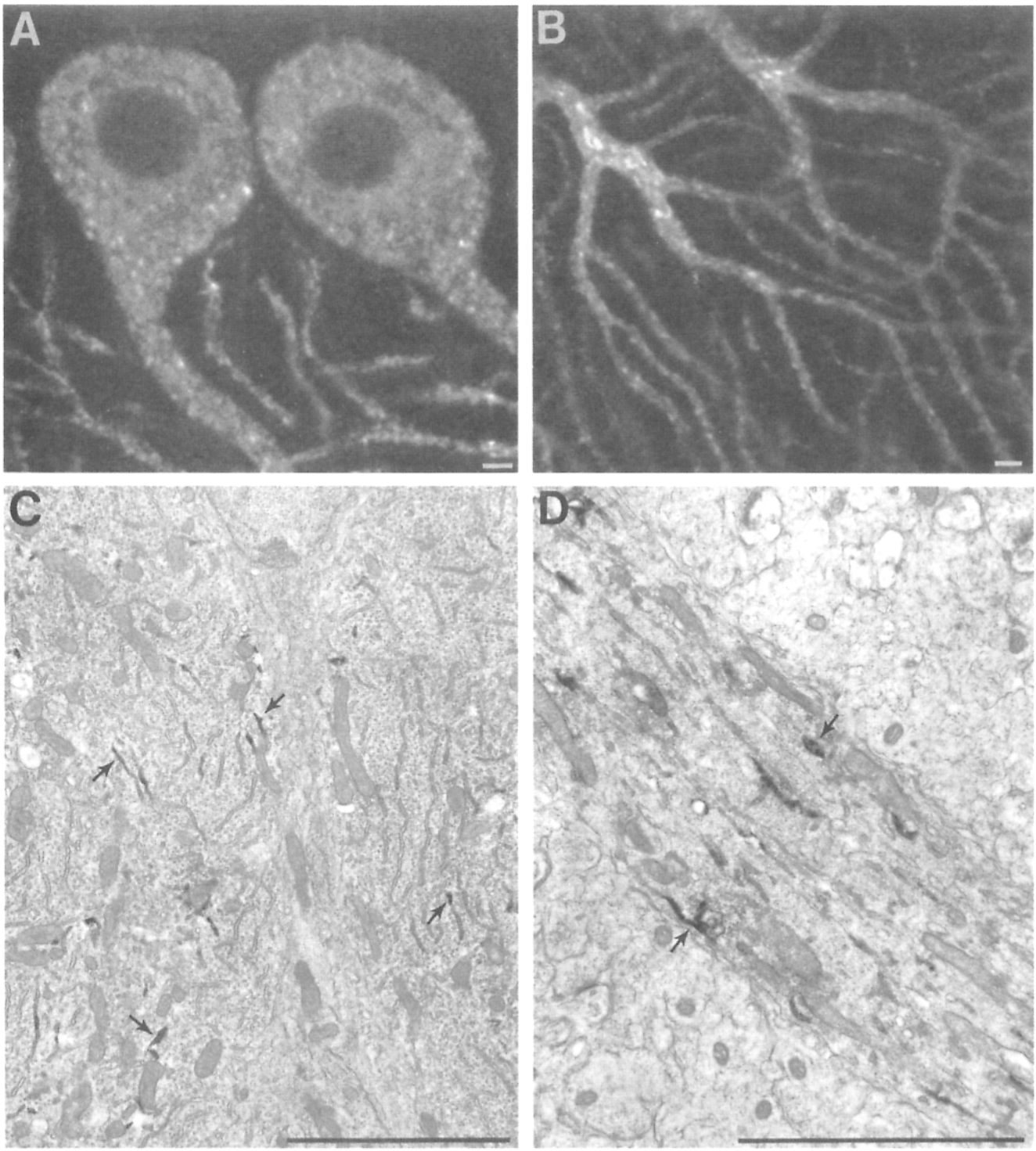

Figure 4. (*A* and *B*) Confocal fluorescence image of chick cerebellar Purkinje cells labeled with rabbit anti-calsequestrin antibodies followed by goat anti-rabbit eosin. Focal staining is observed in the cytoplasm of the Purkinje cell bodies (*A*) and in the dendrites (*B*). Thin section electron micrographs from similarly stained regions of two adjacent Purkinje cell bodies (*C*) and dendrites (*D*) that have undergone fluorescence photooxidation. The reaction product is confined to a portion of the lumen of the endoplasmic reticulum (*arrows*). Bar, 4 μm.

that the rate of photooxidation for a given eosin concentration was independent of the DAB concentration in the tested range, suggesting that the chemical species generated upon illumination of eosin was an effective scavenger of DAB. If the oxygen in solution was displaced with argon before illumination the reaction was completely inhibited (Fig. 1 *D*).

To evaluate and optimize the use of eosin-based immunofluorescent photooxidation for correlated light and electron microscopy, a variety of test specimens were selected. The spatial resolution of the labeling procedure was assessed by evaluating the eosin-based immunolabeling of microtubules. Microtubules within cultured bovine aortic endothelial cells

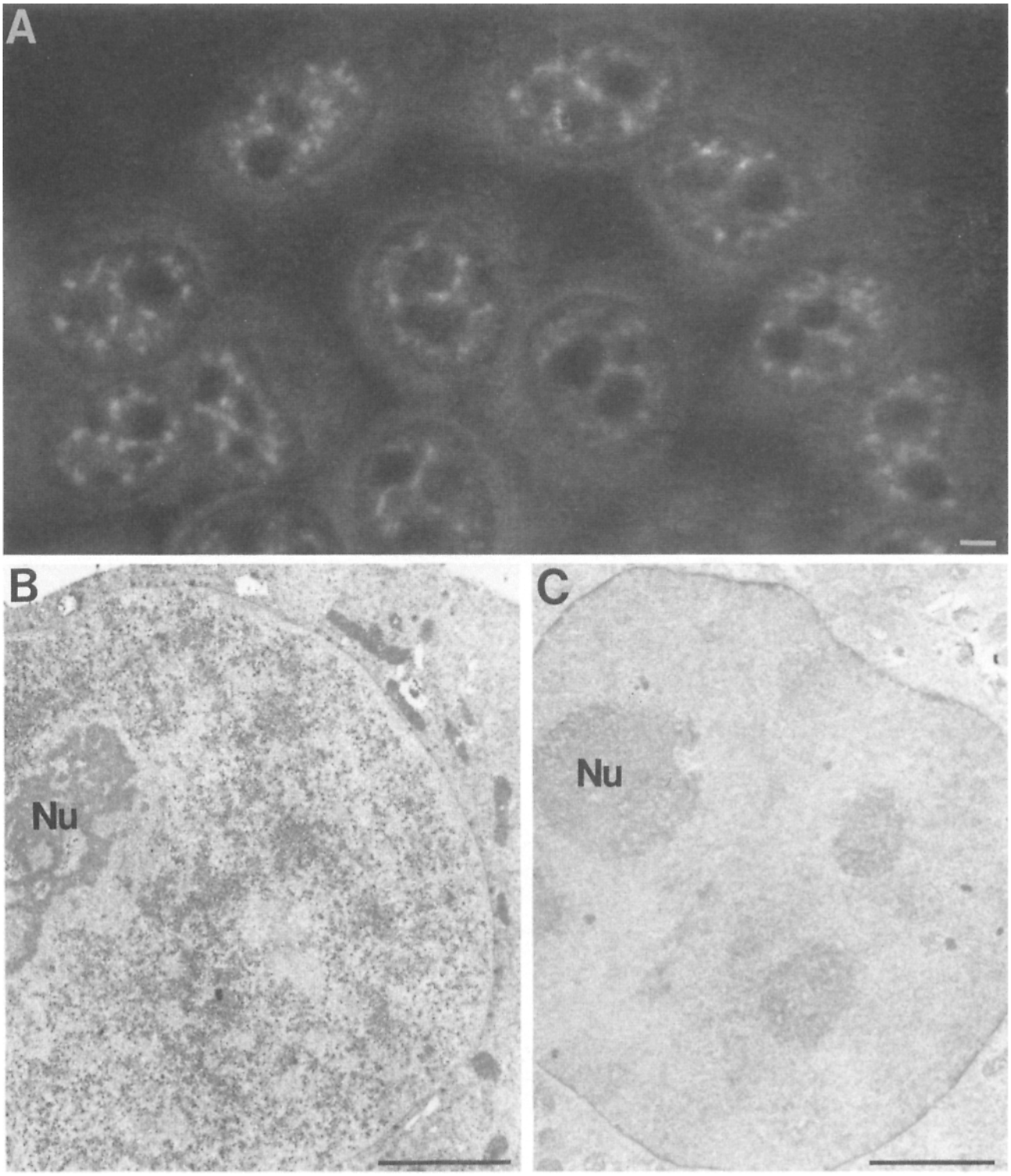

Figure 5. (*A*) Confocal image of HeLa cells labeled for poly(A)$^+$ RNA using in situ hybridization with biotinylated poly-dT and a streptavidin-eosin conjugate. (*B*) Electron micrograph of a thin section showing the distribution of poly(A)$^+$ RNA in the nucleus following fluorescence photooxidation with eosin. (*C*) Electron micrograph of a control cell in which the biotinylated poly-dT probe was omitted. (Nu, nucleolus). Bar, 2.5 μm.

were first reacted with mouse monoclonal antibodies to β-tubulin followed by an anti-mouse IgG–eosin conjugate. These preparations were examined with laser-scanning confocal light microscopy using either 488- or 514-nm excitation. Fig. 2 *A* demonstrates that very high-resolution immunofluorescent images can be obtained with eosin labeling and that individual microtubules may easily be resolved. For photooxidation, the cells were immersed in chilled, oxygenated DAB and the dye was excited for 5–20 min with the 515-nm excitation line from either a 100–200 W mercury or

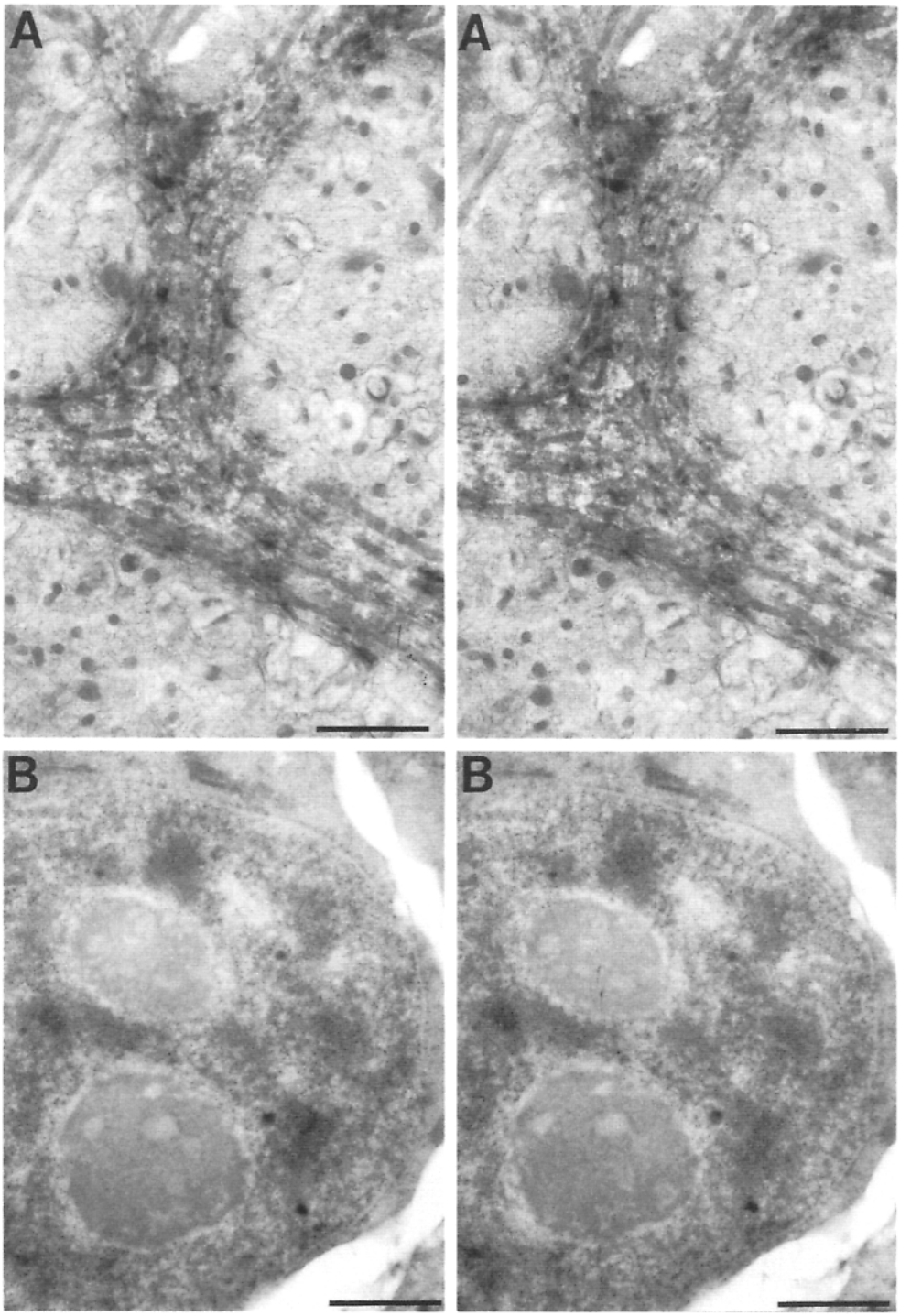

Figure 6. Intermediate voltage electron micrograph stereopairs of 0.5-μm thick sections. (*A*) The 3-dimensional distribution of calsequestrin immunoreactivity in a subset of the dendritic endoplasmic reticulum of a cerebellar Purkinje cell can be seen. (*B*) In 3-dimensions the intranuclear distribution of poly(A)$^+$ RNA in a HeLa cell appears as a complex network with a distinctly non-perinucleolar pattern. Bars: (*A*) 2 μm; (*B*) 2.5 μm.

75 W xenon arc lamp. The amount of time necessary for the reaction was directly related to the relative intensity of both the illumination and the fluorescence brightness. Fig. 2 *B* is a lower magnification fluorescence image of a cell immunolabeled for β-tubulin prior to the addition of DAB. Fig. 2 *C* is a transmitted light image of the same cell after photooxidation for 5 min. A good correspondence can be seen between the fluorescence and transmitted light images.

In contrast to Bentivoglio and Su (1990), we did not find that imaging the area to be photooxidized before the addition of DAB seriously interfered with subsequent photooxidation, as long as photobleaching was kept to a minimum. Antifade media were not used during imaging because we found that they may interfere with subsequent photooxidation in the imaged area. As previously reported (Hulspas et al., 1993), if 4% *n*-propyl gallate or 0.45% triethylenediamine was used as an antifade medium, the phenomenon of fluorescence brightening was observed with eosin labeling as the sample was initially illuminated. If subsequently illuminated in the presence of DAB, regions of the sample that underwent this fluorescence brightening showed only weak photooxidation of DAB compared to surrounding areas (data

not shown). The most likely explanation for this phenomenon is that it is due to the irreversible photodehalogenation of the eosin molecule, yielding a fluorescein-like molecule possessing a higher fluorescence quantum efficiency but with inferior photooxidation properties. For this reason, rather than using these anti-fade media, photobleaching was minimized during fluorescence imaging by deoxygenating the buffer solution with argon gas, and by using the minimum illumination necessary. Under these conditions fluorescence brightening was not observed. Whether this phenomenon would be observed with other anti-fade compounds was not determined.

After photooxidation, cells were postfixed, embedded, and sectioned for electron microscopy. An example of a reacted bovine aortic endothelial cell immunolabeled for β-tubulin is shown in the electron micrographs in Fig. 3 (*A* and *B*). As can be seen from these images, the delineation of individual stained microtubules was excellent. Under optimal reaction conditions the reaction product had a very fine granular structure and exhibited minimal diffusion. The reaction product generated was similar in appearance to that seen with the photooxidation of DAB by Bodipy-ceramide (Takizawa et al., 1993). Fig. 3 *C* is a region of an immunolabeled cell from the same culture plate that was not illuminated and thus no reaction product was formed.

To test the procedure on tissue sections, 80-μm-thick vibratome sections of chicken cerebellum were labeled with an anti-calsequestrin rabbit polyclonal antibody followed by an anti-rabbit IgG–eosin conjugate. Calsequestrin is a calcium-binding protein found within the lumen of the endoplasmic reticulum and was chosen because its distribution presents a serious accessibility problem for immunolabeling. Fig. 4 shows a confocal immunofluorescent image of calsequestrin immunoreactivity in the cell body (Fig. 4 *A*) and in the dendrite (*B*) of Purkinje cells in the cerebellum. Electron micrographs of these same regions following photooxidation are shown in Fig. 4 (*C* and *D*). The lumenal localization of calsequestrin labeling is clearly seen. Despite the relative inaccessibility of the antigen, specific labeling could be seen several microns into the tissue section, even when only low concentrations of detergents were used. The depth of reagent penetration could be assessed directly by confocal microscopy.

Photooxidation with eosin has also been adapted for fluorescence-based in situ hybridization detection of specific nucleic acid sequences. Fig. 5 *A* is a confocal fluorescent image demonstrating the localization of poly(A)$^+$ RNA in HeLa cells hybridized with biotinylated poly-dT followed by a streptavidin–eosin conjugate. In agreement with previous reports (Carter et al., 1991, 1993), the fluorescent labeling of poly(A)$^+$ RNA appeared predominantly as a speckled pattern in the nuclei with weaker diffuse nuclear and cytoplasmic staining. When viewed with the electron microscope following photooxidation (Fig. 5 *B*), the intranuclear staining pattern appeared highly specific and showed excellent correlation to the fluorescence images. No reaction product was observed in preparations where the hybridizing probe was omitted, as seen in Fig. 5 *C*.

The enhanced penetration of the labeling reagents allowed for the examination of the three-dimensional ultrastructural distribution of proteins and specific nucleic acid sequences using high voltage electron microscopy. Fig. 6 *A* is a stereopair of a 0.5-μm-thick section examined at 400 keV illustrating the three-dimensional nature of calsequestrin immunoreactivity in the proximal dendrite of a Purkinje cell. In Fig. 6 *B* the three-dimensional distribution of poly(A)$^+$ RNA can be observed in a stereopair from a 0.5-μm-thick section of a HeLa cell following in situ hybridization and photooxidation. The staining revealed a highly complex, interconnected network in the nucleus with a distinct nonperinucleolar distribution (Fig. 6 *B*).

Technical Considerations

We have tested several variables to determine the optimal conditions for producing rapid photooxidation and good tissue morphology. As expected, the process of photooxidation of DAB is highly oxygen dependent. If the concentration of dissolved oxygen is reduced the reaction is also inhibited. Therefore, it is important to provide an oxygen source for the reaction, particularly for thick tissue sections. This may be accomplished by continuous perfusion of aerated or oxygenated DAB, or in the case of thin monolayers of cells one may simply allow the free exchange of oxygen from the fluid surface by using a thin uncovered layer of solution. For this reason we prefer an inverted microscope to allow use of a high numerical aperture objective lens while the solution is left uncovered. To minimize the spontaneous oxidation of DAB, to increase the saturation point of dissolved oxygen and to minimize diffusion of reaction product, the reaction should be run at <5°C.

The reaction rate is directly related to the frequency and intensity of the illumination and the relative intensity of the fluorescence. Therefore the use of high intensity mercury or xenon light sources and a high numerical aperture objective lens is important. In addition, the excitation filter should be approximately 515 nm with a band width of no more than 40 nm, since illumination with shorter wavelengths may increase the level of background staining.

We have observed that mitochondria can oxidize DAB even in fixed tissue, and can thus contribute a significant source of non-specific staining. This phenomenon may account for the observation of Bentivoglio and Su (1990) that photooxidation can take place even when there is no fluorescence. Fixation with glutaraldehyde and treatment with 0.06 M potassium cyanide following immunolabeling but before photooxidation greatly reduced mitochondrial staining. In many instances brief fixation with glutaraldehyde prior to photooxidation was necessary to achieve good ultrastructural morphology. Without this protection the generated oxygen radicals could severely degrade the ultrastructural preservation. Pretreatment with glutaraldehyde also significantly reduced the diffusion of the reaction product. Fixation of the cells and tissues tested with 2% monomeric glutaraldehyde for several minutes had little or no effect on the specificity and intensity of the eosin fluorescence in the samples tested.

Discussion

We have shown that the fluorescent molecule eosin conjugated to either IgG or streptavidin can be used to produce high quality images using immunofluorescence and fluorescence in situ hybridization and is far superior to fluorescein in the photooxidation of DAB. The use of photooxidation with eosin offers several advantages over other methods for

correlated light and electron microscopy. First, since it is fluorescence based, this procedure takes full advantage of high-resolution confocal light microscopic imaging methods. Second, eosin is a relatively small molecule compared to colloidal gold and peroxidase anti-peroxidase or avidin-biotin complexes (Sternberger, 1986; Hsu et al., 1981). The relatively small size of eosin-antibody conjugates allows for greater penetration into cells and tissues than either gold or enzyme based methods, essentially making the penetration of the primary antibody the limiting factor. This feature is useful for localization of difficult to access antigens and makes it possible to examine the three-dimensional distribution of immunolabeling using correlated confocal and high voltage electron microscopy. Third, under optimal conditions the reaction product generated by this method exhibits a very fine structure, and there appears to be minimal diffusion of the reaction product from the site of production. This is probably due to a number of factors including the very short lifetime of $^1O_2$ in the DAB solution, the high degree of cytosol crosslinking by glutaraldehyde fixation, and the low temperature at which the reaction is run. Thus, in many cases, this method may be useful in place of colloidal gold or enzyme based methods for high resolution protein or nucleic acid sequence localization.

Although the exact process by which photooxidation of DAB occurs is not known, the absolute requirement of oxygen suggests that singlet oxygen may be involved. A role for singlet oxygen is also supported by the observation that β-carotene, a singlet oxygen scavenger, inhibited photooxidation in cultured cells and tissue sections (unpublished observation). A likely reaction mechanism involves the excited singlet state of eosin undergoing the phenomenon of intersystem crossing to the triplet state, and thereby transferring its energy to ground state triplet oxygen ($^3O_2$) to form $^1O_2$. The highly reactive singlet oxygen could then lead to the oxidation of the DAB.

The superiority of eosin in the photooxidation reaction over other fluorescent compounds commonly used for immunofluorescent labeling is likely due to two factors. First, as previously mentioned, eosin is a more efficient generator of $^1O_2$ through the phenomenon of intersystem crossing compared to fluorophores such as fluorescein. Second, the presence of bromine atoms probably allows eosin to resist destruction by its self-generated reactive oxygen species thereby prolonging its ability to produce $^1O_2$. A more thorough understanding of the reaction mechanism by which photooxidation occurs will likely be useful for refining the procedure and for the development of more efficient compounds. Since the addition of bromine atoms results in an increase in Φ_f, one might be tempted to continue further down the periodic table with heavier-atom substitution from tetrabromofluorescein (eosin) to tetraiodofluorescein (erythrosin). However, erythrosin has almost no fluorescence (Φ_f = 0.02) and only slightly higher efficiency of intersystem crossing than eosin (Gandin et al., 1983). A more likely way in which to improve this technique is to exploit the fact that the Φ_f and Φ_{1O_2} of most compounds are highly dependent on the solvent medium. For example, the Φ_f of eosin is threefold higher in ethanol than in water (Fleming et al., 1977) whereas the Φ_{1O_2} is greater in water than ethanol (Gandin et al., 1983). We are currently working to determine the optimal medium for maximizing the fluorescence quantum yield of eosin as well as that for maximizing DAB photooxidation. Another approach worth exploring is the possibility of dual conjugation of both an efficient photooxidizer and a separate fluorophore with differing absorption maxima to the same IgG molecule. This has the potential of allowing fluorescence imaging using one frequency of illumination to excite a high Φ_f fluorophore and then using a different frequency to excite a high Φ_{1O_2} photooxidizer. The feasibility of this approach is also currently being investigated.

We would like to thank Ms. Victoria Edelman for her excellent technical assistance and Dr. Cathy Galbraith for the bovine aortic endothelial cell preparations.

This work was supported by National Institutes of Health grants NS14718, NS26739, and RR04050 to M. H. Ellisman and grant NS27177 and support from the Howard Hughes Medical Institute to R. Y. Tsien.

Received for publication 17 March 1994 and in revised form 16 May 1994.

References

Balercia, G., S. Chen, and M. Bentivoglio. 1992. Electron microscopic analysis of fluorescent neuronal labeling after photoconversion. *J. Neurosci. Methods.* 45:87–98.

Bentivoglio, M., and H. S. Su. 1990. Photoconversion of fluorescent retrograde tracers. *Neurosci. Lett.* 113:127–133.

Carter, K. C., D. Bowman, W. Carrington, K. Fogarty, J. A. McNeil, F. S. Fay, and J. B. Lawrence. 1993. A three-dimensional view of precursor messenger RNA metabolism within the mammalian nucleus. *Science (Wash. DC).* 259:1330–1335.

Carter, K. C., K. L. Taneja, and J. B. Lawrence. 1991. Discrete nuclear domains of poly(A) RNA and their relationship to the functional organization of the nucleus. *J. Cell Biol.* 115:1191–1202.

Conrad, P. A., M. A. Nederlof, I. M. Herman, and D. L. Taylor. 1989. Correlated distribution of actin, myosin, and microtubules at the leading edge of migrating Swiss 3T3 fibroblasts. *Cell Motil. Cytoskeleton.* 14:527–543.

Fleming, G. R., A. W. E. Knight, J. M. Morris, R. J. S. Morrison, and G. W. Robinson. 1977. Picosecond fluorescence studies of xanthene dyes. *J. Am. Chem. Soc.* 99:4306–4311.

Galbraith, C. G. 1994. A structural model of the endothelial cell. Dissertation. University of California, San Diego, La Jolla, CA. 189 pp.

Gandin, E., Y. Lion, and A. Van de Vorst. 1983. Quantum yield of singlet oxygen production by xanthene derivatives. *Photochem. Photobiol.* 37: 271–278.

Hatchard, C. G., and C. A. Parker. 1956. A new sensitive chemical actinometer. II. Potassium ferrioxalate as a standard chemical actinometer. *Proc. R. Soc. Lond. Ser. A.* 235:518–536.

Hsu, S. M., L. Raine, and H. Fanger. 1981. Use of avidin-biotin-peroxidase complex (ABC) in immunoperoxidase techniques: a comparison between ABC and unlabeled antibody (PAP) procedures. *J. Histochem. Cytochem.* 29:577–580.

Hulspas, R., P. J. Krijtenburg, J. F. Keij, and J. G. J. Bauman. 1993. Avidin-EITC: an alternative to avidin-FITC in confocal scanning laser microscopy. *J. Histochem. Cytochem.* 41:1267–1272.

Lubke, J. 1993. Photoconversion of diaminobenzidine with different fluorescent neuronal markers into a light and electron microscopic dense reaction product. *Microsc. Res. Tech.* 24:2–14.

Maranto, A. 1982. Neuronal mapping: a photooxidation reaction makes Lucifer Yellow useful for electron microscopy. *Science (Wash. DC).* 217:953–955.

Pagano, R. E., M. A. Sepanski, and O. C. Martin. 1989. Molecular trapping of fluorescent ceramide analogue at the Golgi apparatus of fixed cells: interaction with endogenous lipids provides a trans-Golgi marker for both light and electron microscopy. *J. Cell Biol.* 109:2067–2079.

Papadopoulos, G. C., and I. Dori. 1993. DiI labeling combined with conventional immuncytochemical techniques for correlated light and electron microscopic studies. *J. Neurosci. Methods.* 46:251–258.

Peters, D. M., L. M. Portz, J. Fullenwider, and D. F. Mosher. 1990. Coassembly of plasma and cellular fibronectins into fibrils in human fibroblast cultures. *J. Cell Biol.* 111:249–256.

Sandell, J. H., and R. H. Masland. 1988. Photoconversion of some fluorescent markers to a diaminobenzidine product. *J. Histochem. Cytochem.* 36: 555–559.

Schmued, L. C. and L. F. Snavely. 1993. Photoconversion and electron microscopic localization of fluorescent axon tracer fluoro-ruby (rhodamine-dextran-amine). *J. Histochem. Cytochem.* 41:777–782.

Sternberger, L. A. 1986. Immunocytochemistry. John Wiley & Sons, Inc., New York. 354 pp.

Takizawa, P. A., J. K. Yucel, B. Velt, D. J. Faulkner, T. Deerinck, G. Soto, M. Ellisman, and V. Malhotra. 1993. Complete vesiculation of Golgi membranes and inhibition of protein transport by a novel sea sponge metabolite, Ilimaquinone. *Cell.* 73:1079–1090.

von Bartheld, C. S., D. E. Cunningham, and E. W. Rubel. 1990. Neuronal tracing with DiI: decalcification, cryosectioning and photoconversion for light and electron microscopic analysis. *J. Histochem. Cytochem.* 38:725–733.